Phosphorus Chemical Shift Tensors for Tetramethyldiphosphine Disulfide: A ^{31}P Single-Crystal NMR, Dipolar-Chemical Shift NMR, and Ab Initio Molecular Orbital Study

Myrlene Gee, Roderick E. Wasylishen,* and Klaus Eichele

Department of Chemistry, Dalhousie University, Halifax, Nova Scotia, Canada, B3H 4J3

James F. Britten

Department of Chemistry, McMaster University, Hamilton, Ontario, Canada, L8S 4M1

Received: December 23, 1999

Phosphorus chemical shift and spin−spin coupling tensors have been characterized for tetramethyldiphosphine disulfide (TMPS) by analysis of ^{31}P CP NMR spectra obtained at 4.7 T for a single crystal. In addition, ^{31}P CP NMR spectra of stationary powder and magic angle spinning (MAS) samples have been acquired at two applied magnetic fields (4.7 and 9.4 T) and analyzed independently using the dipolar-chemical shift method. A 2D spin-echo NMR spectrum was also obtained to independently determine the effective ^{31}P−^{31}P dipolar coupling constant. The crystal structure of TMPS (space group *C*2/*m*) consists of six molecules per unit cell. For two of the six molecules, the two phosphorus nuclei are related by an inversion center (site 1), while the remaining four molecules possess mirror planes containing the S−P−P−S bonds (site 2). The differences between the two sites are very subtle, as revealed by a redetermination of the X-ray crystal structure. The phosphorus chemical shift tensors obtained from both single-crystal and dipolar-chemical shift NMR methods are in excellent agreement. For site 1, $\delta_{11} = 91$ ppm, $\delta_{22} = 75$ ppm, and $\delta_{33} = -63$ ppm with an error of ±2 ppm for each component. The principal components of the phosphorus chemical shift tensor at site 2 are very similar; $\delta_{11} = 92$ ppm, $\delta_{22} = 74$ ppm, and $\delta_{33} = -59$ ppm, again with errors of ±2 ppm. The phosphorus chemical shift tensors for both sites are oriented such that the direction of highest shielding is closest to the P−S bond while the direction of least shielding is perpendicular to the plane containing the S−P−P−S bonds. Ab initio (RHF and DFT) calculations of the phosphorus chemical shift tensors for both sites are in good agreement with experiment.

Introduction

Nuclear magnetic resonance studies of solids provide information that is unavailable from solution studies. For example, solid-state NMR studies offer the opportunity to characterize chemical shift, dipolar coupling, and *J*-coupling tensors as well as quadrupolar coupling interactions for systems involving nuclei with $I > {}^1/_2$. The presence of all these interactions, however, makes the analysis of NMR spectra acquired from solids challenging.[1] The determination of the chemical shift tensor, both its principal components and the orientation of its principal axis system (PAS) with respect to the molecule, is particularly valuable due to its close relationship with the local structure and electronic properties of the molecule.[2] While isotropic chemical shifts have been extensively investigated in solution, trends are often observed which defy simple explanations in terms of local structure, particularly in the case of phosphorus chemical shifts.[3] The characterization of the chemical shift *tensor* for model systems is valuable because it provides essential data necessary for the successful interpretation of chemical shift trends.

The majority of NMR experiments performed on crystalline powder samples do not provide the orientation of the chemical shift tensor; however, the presence of isolated spin pairs allows for the application of the dipolar-chemical shift method in order to obtain some orientation information.[4] In this technique, the orientation of the PAS of the chemical shift tensor is determined relative to the dipolar tensor, which is axially symmetric with the unique axis along the vector between the two nuclei of the spin pair. The details of this method have been well described in the literature.[4−6] In the absence of symmetry,[7] the analysis of 1D NMR spectra of stationary samples requires information about the magnitude of the effective dipolar coupling constant, R_{eff}. It is well documented that reliable values of R_{eff} can be obtained independently from the 2D spin-echo experiment.[5a,8,9]

As a complement to experimental studies, ab initio molecular orbital calculations can be quite valuable for characterizing the chemical shift tensor, particularly for determining the tensor orientation in the molecular frame of reference.[5b,c,10] The progress in first principles calculation of NMR parameters has been reviewed recently.[11] In order to evaluate the accuracy of these methods for characterizing chemical shift tensors, one can compare calculated results with data obtained from single-crystal NMR studies.[5a,10a,b,12] In principle, the latter experiments provide the principal components and orientations of the chemical shift tensors, as well as dipolar and indirect spin−spin coupling tensors. Unfortunately, single crystals of sufficient size and quality are not easily obtained for most compounds; hence, such data are relatively rare in the literature. Recent advances in hardware and software have made the single-crystal NMR experiment more efficient.[1b,13]

An ideal model system for such a comparison of data obtained from single-crystal NMR studies vs data from NMR studies of

* Corresponding author. Tel: (902)-494-2564. Fax: (902)-494-1310. E-mail: Roderick.Wasylishen@dal.ca.

10.1021/jp9944839 CCC: $19.00
Published on Web 04/26/2000

SCHEME 1: Structure of Tetramethyldiphosphine Disulfide, TMPS

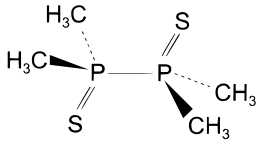

crystalline powder samples and ab initio calculations is tetramethyldiphosphine disulfide, $[(CH_3)_2PS]_2$, abbreviated as TMPS (Scheme 1). It is straightforward to grow a large single crystal of this compound. In addition, the molecule is sufficiently small, allowing for ab initio calculations with acceptably large basis sets and various levels of theory. There have been a few NMR studies of alkyldiphosphine disulfides in the literature, many solution studies stemming from an interest in the relationship between conformation and $^1J(^{31}P,^{31}P)$.[14,15] Tetraethyldiphosphine disulfide[6,16] (TEPS) and tetrabutyldiphosphine disulfide[17] (TBPS) have been a testing ground for the determination of anisotropy in the indirect spin−spin coupling tensors. For TEPS, the upper limit for the anisotropy of $^1J(^{31}P,^{31}P)$, ΔJ, is 462 Hz.[6] However, there are no extensive ab initio studies of phosphorus chemical shielding tensors in the literature for these compounds. Some experimental and ab initio investigations of related compounds, the dithiaphosphetanes, $[RSP(S)S]_2$, and dithioxophosphoranes, RPS_2, have been reported.[18] For $Ag_4P_2O_6$, a significant anisotropy in the $^{31}P,^{31}P$ indirect coupling tensor has been reported, $\Delta J = 800 \pm 80$ Hz.[19]

In this work, we report the phosphorus chemical shift and dipolar coupling tensors for TMPS as characterized by ^{31}P single-crystal NMR. These results are compared with those obtained from an independent analysis of ^{31}P NMR spectra of crystalline powder samples. In addition, the quality of ab initio calculations of phosphorus chemical shift tensors is evaluated by comparison with the experimental results. Finally, our analysis leads to an upper limit of the anisotropy of the $^1J(^{31}P,^{31}P)$ tensor for TMPS.

Experimental Section

A sample of TMPS was obtained from Johnson Matthey Electronics.

Redetermination of X-ray Structure. For reasons discussed below, the X-ray structure of TMPS was redetermined. A single crystal of dimensions 0.02 mm × 0.20 mm × 0.45 mm was selected from a sample of TMPS recrystallized from CH_2Cl_2 and mounted on a glass fiber. X-ray diffraction experiments were carried out on a Siemens P4RA diffractometer (Mo Kα, $\lambda = 0.710\ 69$ Å, graphite monochromator) at room temperature, using the ω and ϕ scan technique with a CCD area detector. The maximum 2θ value was 55.0°. The parameters for the monoclinic cell were $a = 18.860(6)$ Å, $b = 10.693(6)$ Å, $c = 7.021(4)$ Å, and $\beta = 94.608(3)°$, with $Z = 6$. With FW = 186.20, the calculated density is 1.311 g/cm^3. Of the 5143 reflections collected, 1686 were unique. The data were corrected for Lorentz and polarization effects and for absorption using an empirical model.[20] The structure was refined in $C2/m$,[21] where all atoms with the exception of hydrogen atoms were refined anisotropically. Hydrogen atoms in their observed positions were refined isotropically. The final cycle of full-matrix least-squares refinement, using all unique reflections ($I > 3\sigma(I)$) with 101 variable parameters, converged with unweighted and weighted agreement factors of $R = 0.0327$ and $R_w = 0.0706$, respectively. On the final difference Fourier map, the maximum and minimum peaks corresponded to 0.384 and −0.260 electrons Å^{-3}. All calculations were performed with SHELXTL.[22] Structural parameters are given in Table 1 and the atom labeling scheme is shown in Figure 1.

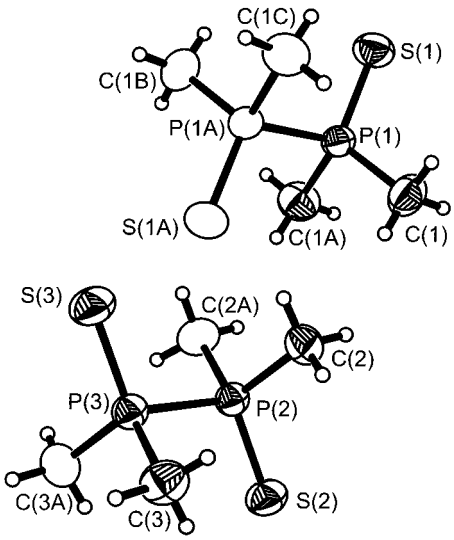

Figure 1. Labeling scheme for the TMPS X-ray structure (see Table 1).

TABLE 1: Selected Bond Lengths (Å) and Bond Angles (deg) for TMPS

site 1		site 2	
P(1)−P(1A)	2.2137(14)	P(2)−P(3)	2.2144(10)
S(1)−P(1)	1.9569(11)	S(2)−P(2)	1.9596(10)
P(1)−C(1)	1.799(3)	S(3)−P(3)	1.9560(11)
P(1)−C(1A)	1.799(3)	P(2)−C(2)	1.796(2)
C(1)−P(1)−C(1A)	105.7(2)	P(2)−C(2A)	1.796(2)
C(1A)-P(1)−S(1)	115.50(11)	P(3)−C(3)	1.803(3)
C(1)−P(1)−P(1A)	103.56(10)	P(3)−C(3A)	1.803(3)
S(1)−P(1)−P(1A)	111.65(5)	C(2)−P(2)−S(2)	115.35(9)
		C(3)−P(3)−S(3)	115.25(10)
		C(2)−P(2)−P(3)	103.90(9)
		S(2)−P(2)−P(3)	111.58(4)
		C(3)−P(3)−P(2)	104.02(10)
		S(3)−P(3)−P(2)	111.11(5)
		C(2)−P(2)−C(2A)	105.5(2)
		C(3)−P(3)−C(3A)	106.0(2)

TABLE 2: Direction Cosines to Orient the Monoclinic Crystal Axes (*a, b, c*) with Respect to the Orthogonal NMR Cube Frame (*X, Y, Z*) As Determined by X-ray Diffraction

	X	*Y*	*Z*
a	0.9972	0.0398	−0.0446
b	−0.0525	0.9980	−0.0458
c	−0.0268	0.0458	0.9983

Phosphorus-31 Single-Crystal NMR. A large single crystal of TMPS, grown in CH_2Cl_2 with dimensions of approximately 3 mm × 3 mm × 3.7 mm, was glued into the corner of a hollow three-sided crystal holder, made from aluminum oxide, measuring 4 mm on each side. X-ray diffraction methods were used to determine the orientation of the monoclinic crystal system with respect to the cube axes (Table 2). The cell axes were orthogonalized using Rollett's convention.[23] The rotation matrix, $\mathbf{R}_z(\gamma)\mathbf{R}_y(\beta)\mathbf{R}_z(\alpha)$,[24] relates the orthogonalized crystal system and the cube frame of reference. For our sample, $\alpha = 120.33°$, $\beta = 3.04°$, and $\gamma = 242.72°$. Phosphorus-31 NMR data from the single crystal were obtained on a Bruker MSL 200 spectrometer (4.7 T, corresponding to a ^{31}P NMR frequency of 81.03 MHz), using an automated single-crystal goniometer probe manufactured by Doty Scientific. Rotations were performed about each of the cube's *X*, *Y*, and *Z* axes from 0° to 180° in 9° increments.

All ^{31}P NMR spectra were acquired using cross polarization (CP) under the Hartmann−Hahn match condition. A ^{1}H $\pi/2$ pulse width of 3.1 μs, contact time of 5.0 ms, and a recycle delay of 6 s were used. For each spectrum, 64 transients were adequate to obtain a good signal-to-noise ratio. All spectra are referenced to 85% H_3PO_4(aq). The peaks in each spectrum were fitted with a Gaussian function to obtain the frequencies of the peak maxima. The NMR data for each site were analyzed by linear least-squares fit to

$$f_i(\psi) = A_i + B_i \cos 2\psi + C_i \sin 2\psi \qquad (1)$$

where f_i is the NMR parameter of interest and ψ tracks the rotation angle of the crystal in the goniometer about the ith axis ($i = X, Y, Z$). For the ^{31}P chemical shift data of each site, the position at the center of each doublet was plotted. In the analysis of the ^{31}P−^{31}P dipolar coupling interaction, the splitting between the doublets was plotted for both sites. Phase angles of −2° for the X rotation, −3° for the Y rotation, and −6° for the Z rotation were introduced in order to compensate for errors in the initial goniometer positions. The standard analysis of single-crystal NMR data is described elsewhere.[5a,25]

Phosphorus-31 NMR of Powder Samples. Phosphorus-31 CP NMR spectra of stationary powdered samples and with magic angle spinning (MAS) were acquired on a Bruker MSL 200 and a Chemagnetics CMX Infinity 200 (4.7 T for both, corresponding to a frequency of 81.03 MHz for ^{31}P) and a Bruker AMX 400 (9.4 T, corresponding to a frequency of 161.90 MHz for ^{31}P). Double-air bearing MAS probes were used throughout. Samples were packed into 7 mm (MSL), 7.5 mm (Infinity), and 4 mm (AMX) o.d. zirconium oxide rotors. Typical parameters were ^{1}H $\pi/2$ pulse widths of 4 μs, contact times of 1 ms, and recycle delays of 4 s for MAS samples while 8 s was used for stationary samples. All spectra were referenced to 85% H_3PO_4(aq) by using solid $NH_4H_2PO_4$ which has an isotropic phosphorus chemical shift of 0.81 ppm from 85% H_3PO_4(aq). Phosphorus-31 NMR spectra of stationary samples were simulated using WSOLIDS, a program developed in this laboratory which incorporates the POWDER routine of Alderman et al.[26] NMR spectra of MAS samples were calculated using NMR-LAB,[27] which uses the Monte Carlo method to sample crystal orientations for powder averaging. In our calculations 10 000 orientations were used for the powder averaging. The 2D spin-echo NMR spectrum was acquired on the CMX Infinity 200, using a standard spin-echo pulse sequence with the phase cycling of Rance and Byrd.[28] The experimental parameters were similar to those used for the 1D experiments. The data size for the 2D FT was 512 × 128. Gaussian line broadening of 100 Hz was applied to both dimensions; then the data were processed in magnitude mode. The F1 projection of the 2D spectrum was simulated using SpinEcho, a program developed in this laboratory.

Computational Details. Ab initio calculations were performed using the Gaussian 98 suite of programs[29] running on an IBM RISC/6000 computer. The phosphorus chemical shielding was calculated using the atomic coordinates from the X-ray structure determined in this work. Calculations were performed at the restricted Hartree−Fock (RHF) level of theory as well as with density functional theory (DFT). The gauge-independent atomic orbitals method[30] (GIAO) was used throughout. To compare calculated results with experimental results, the calculated phosphorus chemical shielding was converted to chemical shift using the absolute shielding of 328.35 ppm for the phosphorus nucleus in the reference, 85% H_3PO_4(aq).[31]

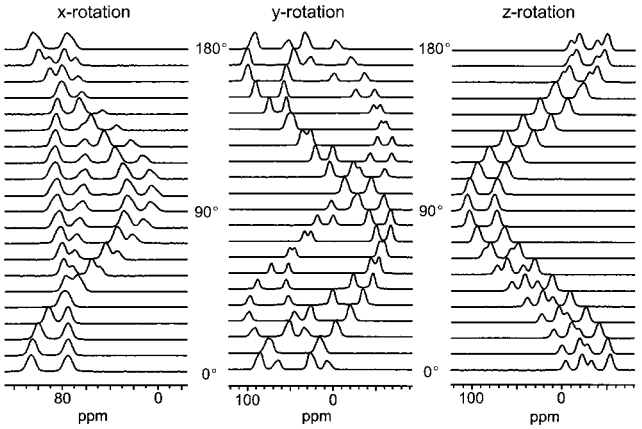

Figure 2. Phosphorus-31 CP NMR spectra of a single crystal of TMPS for rotations of the crystal holder about its *X*, *Y*, and *Z* axes, acquired at 4.7 T.

Results

Phosphorus-31 NMR of a Single Crystal of TMPS. The ^{31}P NMR spectra obtained from a single crystal of TMPS are shown in Figure 2. The X-ray structure of TMPS indicates the presence of six molecules in the unit cell. In two of the six molecules, the two phosphorus nuclei are related by inversion symmetry; hence they are crystallographically and magnetically equivalent, i.e., they form an A_2 spin pair (site 1).[32] In the single-crystal NMR study, site 1 gives rise to a doublet where the splitting is the ^{31}P−^{31}P effective spin−spin coupling at that particular orientation of the crystal in the applied magnetic field, $\mathbf{B}_0$. Since $|^{1}J(^{31}\mathrm{P},^{31}\mathrm{P})|$ is less than 20 Hz,[15] the splitting is given by $3R_{\mathrm{eff}}(3\cos^2\zeta - 1)/2$ where R_{eff} is the effective dipolar coupling constant, $R_{\mathrm{DD}} - {}^{1}/_{3}\Delta J$, and ζ is the angle between the internuclear vector, $\mathbf{r}_{\mathrm{AB}}$ and $\mathbf{B}_0$. The dipolar coupling constant, R_{DD}, is $(\mu_0/4\pi)(\hbar/2\pi)\gamma_{\mathrm{P}}^2\langle r_{\mathrm{PP}}^{-3}\rangle$, where $\langle r_{\mathrm{PP}}\rangle$ is the motionally averaged P−P separation; hence, one can obtain a good estimate of R_{DD} from the X-ray structure. The anisotropy in the J-coupling, ΔJ, is $J_{\parallel} - J_{\perp}$ for the case of an axially symmetric J-coupling tensor.[33]

The remaining four molecules in the unit cell of TMPS possess mirror planes that include the S−P−P−S plane; however, the ^{31}P nuclei are not related by a center of inversion; hence, the two phosphorus nuclei are not crystallographically equivalent. Such a spin pair may be labeled as an AB spin system. In general, AB spin systems give rise to four transitions in the solid state:[4−6,34]

$$\nu_1 = \frac{1}{2}(\nu_{\mathrm{A}} + \nu_{\mathrm{B}} - A - D) \qquad P_1 = 1 - \frac{B}{D} \qquad (2)$$

$$\nu_2 = \frac{1}{2}(\nu_{\mathrm{A}} + \nu_{\mathrm{B}} + A - D) \qquad P_2 = 1 + \frac{B}{D} \qquad (3)$$

$$\nu_3 = \frac{1}{2}(\nu_{\mathrm{A}} + \nu_{\mathrm{B}} - A + D) \qquad P_3 = 1 + \frac{B}{D} \qquad (4)$$

$$\nu_4 = \frac{1}{2}(\nu_{\mathrm{A}} + \nu_{\mathrm{B}} + A + D) \qquad P_4 = 1 - \frac{B}{D} \qquad (5)$$

where ν_{A} and ν_{B} depend on the Larmor frequency, ν_0, the principal components of the chemical shielding tensor, σ_{11}, σ_{22} and σ_{33}, and the orientation of its principal axis system (PAS) with respect to $\mathbf{B}_0$, given by the polar angles θ and ϕ (i is the label for the nucleus of interest):

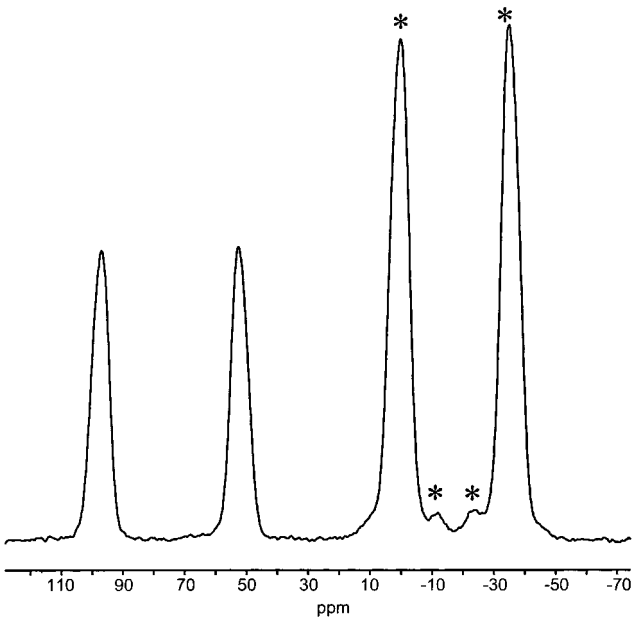

Figure 3. Example of a ^{31}P NMR spectrum of the TMPS single crystal (from the rotation about the *Y* axis of the crystal holder, at 36° from the initial position). The asterisks indicate the four peaks attributed to site 2.

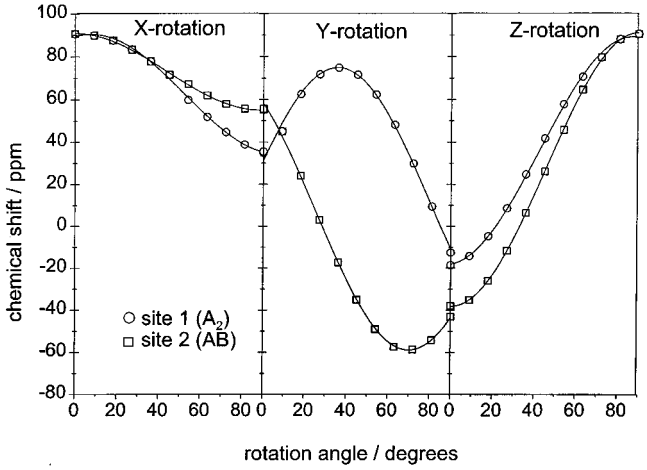

Figure 4. Phosphorus chemical shift as a function of rotation angle for site 1 and site 2. The curves represent the linear least-squares best fit to the experimental data.

$$\nu_i(\theta,\phi) = \nu_0[1 - (\sigma^i_{11}\sin^2\theta\cos^2\phi + \sigma^i_{22}\sin^2\theta\sin^2\phi + \sigma^i_{33}\cos^2\theta)] \quad (6)$$

The terms *A*, *B*, and *D* are

$$A = J_{iso} - R_{eff}(3\cos^2\zeta - 1) \quad (7)$$

$$B = J_{iso} + \frac{1}{2}R_{eff}(3\cos^2\zeta - 1) \quad (8)$$

$$D = [(\nu_A - \nu_B)^2 + B^2]^{1/2} \quad (9)$$

In most of the NMR spectra of the TMPS single crystal (Figure 2), four peaks are evident. The two of lesser intensity are assigned to site 1 and the more intense set is assigned to site 2 since the two sites are present in a 1:2 ratio. It is not obvious in Figure 2 that site 2 is an AB spin system, since the expected four transitions are not immediately apparent. In fact,

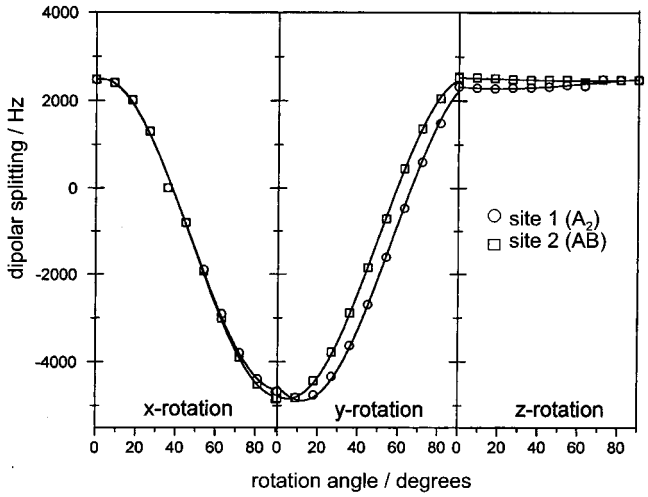

Figure 5. Dipolar splitting as a function of rotation angle for site 1 and site 2. The curves represent the linear least-squares best fit to the experimental data.

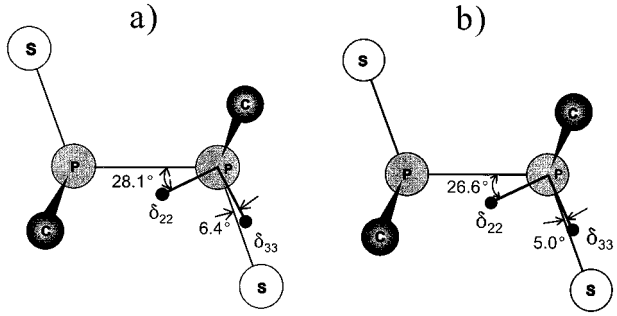

Figure 6. Orientation of the phosphorus chemical shift tensor for TMPS as determined by (a) a single-crystal NMR study and (b) ab initio (RHF) calculations. The orientations are shown for site 1. The plane of the page contains the S−P−P−S moiety. In both cases, δ_{11} is approximately perpendicular to the plane of the page.

very few of the rotations produce NMR spectra where there is any evidence of an AB quartet; one example is shown in Figure 3. Since there are insufficient data to analyze site 2 as an AB spin system, it has been analyzed as an A_2 spin system. The plots of the chemical shift and the dipolar splitting as a function of crystal rotation are shown in Figures 4 and 5, respectively. For the chemical shift tensors, the coefficients of the linear least-squares fit to eq 1 are given in Table 3. The principal components of the chemical shift tensors, δ_{11}, δ_{22}, and δ_{33}, and their respective direction cosines relative to the orthogonalized crystal frame of reference are given in Table 4. The principal components are also summarized in Table 5. As is evident in this table, the phosphorus chemical shift tensor principal components for sites 1 and 2 are virtually identical. Besides presenting the three principal components, the chemical shift tensor is also described in terms of three derived parameters: the isotropic chemical shift, $\delta_{iso} = (\delta_{11} + \delta_{22} + \delta_{33})/3$, the span, $\Omega = \delta_{11} - \delta_{33}$, and the skew, $\kappa = 3(\delta_{22} - \delta_{iso})/\Omega$.[35] The orientation of the tensor is illustrated in Figure 6a for site 1. The direction of highest shielding is closest to the P−S bond, while δ_{11}, the direction of least shielding, is approximately perpendicular to the plane containing the SPPS bonds, with a P−P−δ_{11} angle of 83°. The chemical shift tensor orientation at the other phosphorus nucleus of site 1 is simply an inversion of the one shown in Figure 6a. For site 2, the phosphorus chemical shift tensor is oriented in a similar fashion with respect to the molecule, with δ_{33} at 2.5° from the P−S bond and the P−P−δ_{11} angle of 100°. The presence of a mirror plane in site

TABLE 3: Linear Least-Squares Coefficients for the Phosphorus Chemical Shift and Spin−Spin Coupling Interactions in TMPS as Functions of Crystal Rotation about the Cube *X, Y, Z* Axes[a]

	rotation	A_i	B_i	C_i
		Site 1 (A_2)		
CS[b]	*X*	60.2(42)	26.9(59)	8.8(61)
	Y	7.4(56)	25.8(77)	62.9(80)
	Z	34.7(51)	−53.4(71)	17.8(74)
spin−spin coupling[c]	*X*	−1369(49.0)	3539(67.7)	478.4(70.9)
	Y	−1147(16.7)	−3499(23.1)	−1208(24.2)
	Z	2410(7.3)	−88.7(10.1)	−65(10.5)
		Site 2 (AB)		
CS[b]	*X*	72.0(16)	17.7(22)	−0.3(23)
	Y	8.0(37)	47.5(51)	−48(53)
	Z	27.4(25)	−62.5(34)	11.8(36)
spin−spin coupling[c]	*X*	−1449(44.0)	3615(60.8)	524(63.6)
	Y	−1112(22.4)	−3701(30.9	−367(32.3)
	Z	2490(4.1)	13(5.7)	−10(5.96)

[a] The phase angles for the best fit to the experimental data are −2° for *X*, −3° for *Y*, and −6° for *Z*. [b] Units of ppm. [c] Units of Hz.

TABLE 4: Principal Components and Orientations (Direction Cosines) of the Phosphorus Chemical Shift and Dipolar Coupling Tensors Relative to the Orthogonalized Crystal Axes (*a*bc*) for TMPS

		*a**	*b*	*c*
		Site 1 (A_2)		
δ_{11}/ppm	90.6	−0.1417	0.9836	0.1140
δ_{22}/ppm	74.9	−0.5171	−0.1717	0.8385
δ_{33}/ppm	−63.2	0.8441	0.0598	0.5328
D_{11}/Hz	2538	0.9805	−0.1405	0.1373
D_{22}/Hz	2365	0.1430	0.9897	−0.0080
D_{33}/Hz	−5008	−0.1348	0.02753	0.9905
		Site 2 (AB)		
δ_{11}/ppm	91.8	−0.1120	0.9795	−0.1621
δ_{22}/ppm	74.4	0.3955	0.1964	0.8971
δ_{33}/ppm	−58.8	0.9106	0.0435	−0.4110
D_{11}/Hz	2566	0.9916	−0.1273	0.0236
D_{22}/Hz	2358	0.1280	0.9946	−0.0238
D_{33}/Hz	−4994	−0.0204	0.0268	0.9994

2 requires that the P−P−δ_{11} angle be exactly 90°; however, the magnitudes of δ_{11} and δ_{22} are similar, and thus it is difficult to determine their orientations independently.[6]

The dipolar coupling tensor principal components are given in Table 4 with their respective direction cosines. The spin−spin coupling data for TMPS are summarized in Table 6. In principle, the dipolar coupling tensor in its principal axis system, **D**, is axially symmetric and traceless, with the unique axis along the internuclear vector. For an A_2 spin system

$$\mathbf{D} \equiv \begin{bmatrix} D & 0 & 0 \\ 0 & D & 0 \\ 0 & 0 & -2D \end{bmatrix} = \begin{bmatrix} {}^3/_2 R_{\mathrm{eff}} & 0 & 0 \\ 0 & {}^3/_2 R_{\mathrm{eff}} & 0 \\ 0 & 0 & -3R_{\mathrm{eff}} \end{bmatrix} \quad (10)$$

The nonzero trace and very slight nonaxial symmetry of our dipolar coupling tensors is likely a consequence of experimental errors in the single-crystal NMR experiment. In addition, molecular motion may contribute.[33,36] The experimental values of R_{eff} are 1.669 ± 0.05 kHz for site 1 and 1.665 ± 0.05 kHz for site 2, determined by averaging R_{eff} obtained from each of the diagonal components of **D** (Table 4). The rotation plot for the dipolar splitting (Figure 5) indicates that the unique axis of the dipolar tensor, which is along the P−P bond, is very close to the *Z*-axis of the cube, since the dipolar splitting for both sites is essentially invariant to rotation of the crystal about that axis. This implies that the internuclear vector and $\mathbf{B}_0$ are approximately perpendicular ($\zeta = 90°$) during the rotation about the *Z* axis; hence, a splitting of $^3/_2 R_{\mathrm{eff}}$ is observed.

TABLE 5: Principal Components, Ω, and the Phosphorus Chemical Shift Tensors for TMPS (Determined Experimentally and by ab Initio Calculation)

	δ_{iso}/ppm	δ_{11}/ppm	δ_{22}/ppm	δ_{33}/ppm	Ω/ppm[a]	κ[a]
single crystal						
site 1	34.3	91	75	−63	154	0.79
site 2	35.7	92	74	−59	151	0.76
stationary powder (4.7 T, 9.4 T)						
site 1	34.3	91[b]	75	−63	154	0.79
site 2	36.0	91	76	−59	150	0.80
MAS powder (4.7 T, 9.4 T)[c]						
site 1	34.9					
site 2[c]	37.0					
	37.4					
RHF/6-311G**						
site 1	−19	41	17	−114	155	0.69
site 2[d]	−19	41	18	−115	156	0.71
	−17	42	17	−111	153	0.66
RHF/ 6-311G(3df,3pd)						
site 1	10	66	56	−93	159	0.88
site 2[d]	10	67	58	−94	161	0.89
	11	67	57	−90	157	0.89
B3LYP/ 6-311G(d,p)						
site 1	52	132	97	−74	206	0.66
site 2[d]	50	131	98	−79	210	0.69
	52	132	97	−74	206	0.66

[a] $\Omega = \delta_{11} - \delta_{33}$; $\kappa = 3(\delta_{22} - \delta_{\mathrm{iso}})/\Omega$. [b] Experimental error on the principal components is ±2 ppm. [c] Experimental error on δ_{iso} for site 1 is ±0.03 ppm and ±0.04 ppm for site 2. [d] There are two crystallographically nonequivalent phosphorus nuclei in site 2, hence two sets of principal components are given.

TABLE 6: Spin−Spin Coupling Data for TMPS[a]

method	D_{iso}	R_{eff}	R_{DD}	$\lvert J_{\mathrm{iso}}\rvert$	ΔJ
single crystal					
site 1 (A_2)	−35	1669[b]	1818	18.7[c]	447
site 2(AB)	−23	1665[b]	1816		453
2D spin echo		1690[d]			

[a] All quantities given in units of Hz. [b] Estimated experimental error is ±50 Hz. [c] From ref 15. [d] Experimental error is ±80 Hz.

From R_{DD} calculated using the P−P bond lengths reported in the X-ray crystal structure[37] and R_{eff} determined experimentally, one can estimate ΔJ.[33] The most recently published crystal structure of TMPS[37] reports a significant and unexplained difference in the P−P bond lengths of sites 1 and 2, $r = 2.245(6)$ Å and $r = 2.161(4)$ Å, respectively, resulting in $R_{\mathrm{DD}} = 1.74 \pm 0.04$ kHz and $\Delta J = 0.3 \pm 0.2$ kHz for site 1, while $R_{\mathrm{DD}} = 1.95 \pm 0.03$ kHz and $\Delta J = 0.9 \pm 0.2$ kHz for site 2. This is clearly

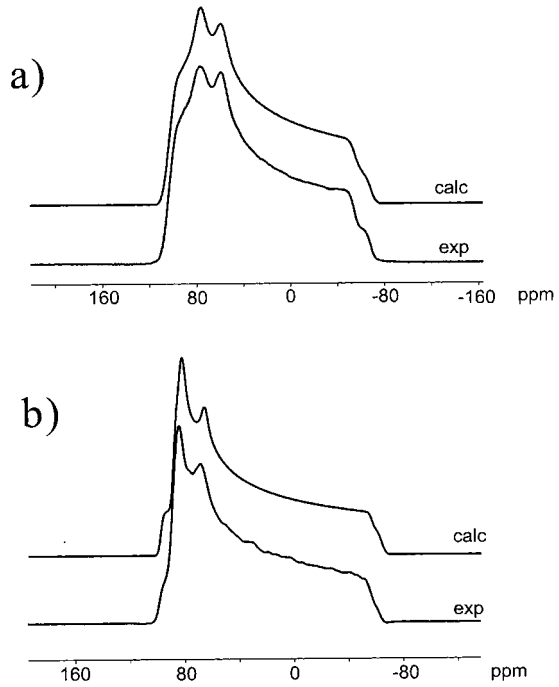

Figure 7. Experimental and calculated ^{31}P CP NMR spectra of stationary powder samples of TMPS, acquired at (a) 4.7 T and (b) 9.4 T. The same experimental NMR parameters were used to simulate the observed spectra at both fields.

suspicious, prompting our redetermination of the X-ray crystal structure. From our investigation, the general features of the X-ray structure are similar to those previously reported; however, the difference in the geometry between the two sites is much less dramatic. The P−P bond lengths from our X-ray data are 2.2173(14) Å and 2.2144(10) Å, for site 1 and site 2 respectively, resulting in more reasonable values of R_{DD} (Table 6). For site 2, the major structural difference between the two $(CH_3)PS$ moieties is the C−P−C bond angle (106.0(2)° vs 105.5(2)°; see Table 1). Using our values of R_{DD} for both sites, the upper limit on ΔJ is approximately 450 Hz. In addition, there may also be a contribution from librational motion of the molecule, which results in a smaller observed value for the dipolar coupling constant.[4b,38] In the absence of an accurate potential energy surface for the P−P vector, a realistic correction of R_{DD} for librational motion is difficult.

Phosphorus-31 NMR Spectra of Crystalline Powder Samples. The ^{31}P NMR spectra of powder samples of TMPS were analyzed independently of the single-crystal work. Before analyzing the ^{31}P NMR spectra of stationary (Figure 7) and MAS (Figure 8) crystalline powder samples of TMPS, the effective dipolar coupling constant can be measured independently using the 2D spin echo experiment.[9] From simulations of the F1 projection (Figure 9) of the 2D spin echo NMR spectrum, $R_{eff} = 1.69 \pm 0.08$ kHz, in good agreement with the single-crystal data. In the simulations, it is assumed that $|^1J(^{31}P,^{31}P)| = 18.7$ Hz which is the value measured in previous solution NMR studies.[15]

The NMR spectra of the stationary samples (Figure 7) are simulated using the above value of R_{eff} to obtain the chemical shift tensor principal components given in Table 5 and tensor orientation information discussed below. The NMR spectra of MAS samples (Figure 8) were calculated using the same parameters as obtained from the stationary samples, with the exception of the isotropic phosphorus chemical shifts for both site 1 and 2. More accurate isotropic chemical shifts are available from the ^{31}P MAS NMR spectra. For site 1, $\delta_{iso} = 34.9$ ppm

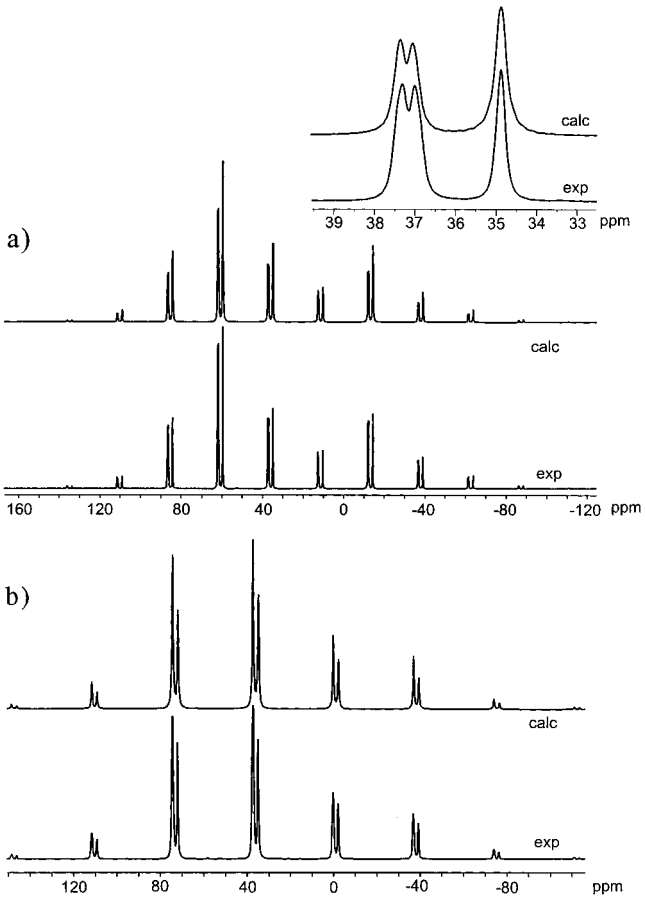

Figure 8. Experimental and calculated ^{31}P MAS NMR spectra of TMPS acquired at (a) 9.4 T with the sample spinning at 3.01 kHz. The inset shows details of the isotropic region. The bottom spectrum (b) was obtained at 4.7 T with the sample spinning at 4.00 kHz.

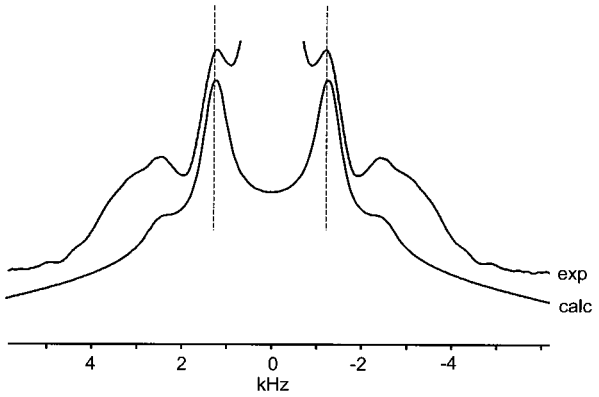

Figure 9. Experimental and calculated F1 projection of the 2D spin-echo ^{31}P NMR spectrum acquired at 4.7 T. The large center peak (truncated in this figure) is an experimental artifact.

while for site 2, the two peaks evident at 9.4 T are at 37.4 and 37.0 ppm (Figure 8), giving a difference of 0.4 ppm between the two phosphorus chemical shifts. The ^{31}P MAS NMR spectra can be successfully simulated based on this information and the data obtained from the simulation of the NMR spectra of stationary samples. Since the single-crystal NMR spectra showed very little AB character, the subtle difference between the nonequivalent phosphorus environments in site 2 was not apparent from that analysis. While one can, in principle, fit the ^{31}P MAS NMR spectra to obtain all the chemical shift and coupling information, these MAS spectra (Figure 8) are essentially featureless, and hence it was necessary to also analyze the NMR spectra of stationary samples, acquired at different

applied magnetic fields (Figure 7). In addition, one cannot apply the Herzfeld−Berger approach[39] to the spinning sideband manifold of the MAS spectra due to the presence of strong dipolar coupling.[40]

In addition to obtaining the principal components of the phosphorus chemical shift tensors, some tensor orientation information is available from the analysis of NMR spectra of powders containing isolated spin pairs[4−6] such as those in TMPS. The orientations are commonly described in terms of Euler angles, α, β, and γ.[41] The angle β gives the position of δ_{33} with respect to the P−P bond, while the difference between the α angles of each tensor, Δα, gives the torsion angle between the respective δ_{33} components. Since the dipolar tensor is axially symmetric, the NMR spectra are invariant to simultaneous rotation of the two phosphorus chemical shift tensors about the P−P bond; hence, only Δα is determined. The angle γ determines whether δ_{11} or δ_{22} lies closest to the P−P bond. The ^{31}P NMR spectra of stationary samples (Figure 7) were successfully simulated using $\Delta\alpha = 0°$ for both site 1 and 2, indicating that the most shielded components of the adjacent phosphorus nuclei lie in the same plane. The angle between the most shielded component and the P−P bond, β, is 63° ± 3° for site 1 and 65° ± 3° for site 2, equally well described by the supplement angles, 117° and 115°, respectively. The orientation of the principal components of the phosphorus shielding tensor obtained from a dipolar-chemical shift analysis is clearly consistent with the single-crystal NMR results.

Ab Initio Calculation of Chemical Shielding Tensors. The calculated principal components of the phosphorus shielding tensors for TMPS are given in Table 5, and the orientation for one phosphorus nucleus in site 1 is shown in Figure 6b. The calculated phosphorus chemical shift tensor orientations for site 2 are similar. Using the 6-311G** basis set, the RHF results for δ_{iso} are about 53 ppm too shielded for both sites; however, the line shapes, described by Ω and κ, are remarkably accurate. Increasing the size of the basis set to 6-311++G(3df,3pd) improves the calculated value of δ_{iso}; however, it is still too shielded by about 24 ppm for both sites. The DFT values are too deshielded by only 16 ppm, but the span is overestimated. Differences between the isotropic chemical shift measured in the solid state compared to ab initio calculations are expected since the calculations are performed on an isolated molecule. The intermolecular effects may be substantial. For example, the phosphorus nucleus in PH_3 is less shielded by 28 ppm in the liquid state compared to the gas state.[31] This is a general trend that nuclei in the gas phase are invariably shielded compared to the condensed phase.[42] The ab initio methods reproduce phosphorus shielding tensor orientations quite well (Figure 6). A series of calculations on H_2PPH_2 indicates that the orientation of the chemical shielding tensor is relatively insensitive to the ab initio method.[43]

Discussion

The phosphorus chemical shift and spin−spin coupling tensors for TMPS obtained by analysis of ^{31}P NMR spectra of crystalline powder samples are in excellent agreement with the single-crystal NMR study. The value of R_{eff} measured by both single-crystal NMR and the 2D spin echo experiment compared to R_{DD} calculated from P−P bond lengths places an upper limit on the anisotropy of the *J* tensor (about 450 Hz), substantially smaller than originally estimated for similar compounds.[16,17] The phosphorus chemical shift tensors obtained from both single-crystal and powder methods are virtually identical. In addition, studies of MAS samples at 9.4 T provide additional details regarding the chemically nonequivalent phosphorus nuclei of site 2. From the analysis of the NMR spectra of stationary powder samples, the principal components of the phosphorus chemical shift tensors are determined. The orientations of the most shielded components relative to the P−P bond as well as to each other are obtained. For both site 1 and site 2, the most shielded components lie in the same plane and are closest to the P−S bond. Unfortunately, the orientation of the tensor in the molecular frame of reference cannot be determined by powder NMR methods. The full tensor orientation is available experimentally from the single-crystal NMR study (Figure 6a). The orientation information obtained from the powder methods is consistent with the single-crystal results.

TABLE 7: Comparison of δ_{iso} and C−P−C Bond Angle for $[R_2P(S)]_2$

R	δ_{iso}/ ppm	δ_{11}/ ppm	δ_{22}/ ppm	δ_{33}/ ppm	C−P−C/ deg
methyl (site 1)[a]	34.1	91	75	−63	105.7(2)
ethyl[b]	50.7	108	98	−54	107.52(9)
n-propyl[c]	45.9				107.8(2)
n-butyl (multiple sites)[d]	49.5	104.7	97.5	−53.7	
	49.7	106.3	96	−53.1	

[a] This work. [b] Reference 6. [c] NMR data from ref 15, X-ray crystal structure from ref 44. [d] NMR data from ref 17, no crystal structure available.

The ab initio methods employed in this work produce line shapes that are in good agreement with experimental results. In addition, the calculated chemical shielding tensor orientations are almost identical to those obtained from the single-crystal NMR study (Figure 6). The invariance of the chemical shielding tensor orientation with method suggests that calculations at the Hartree−Fock level with moderate-sized basis sets are adequate for obtaining the tensor orientation. This is particularly useful for large systems, where high-level calculations are very difficult due to limited computational resources.

It has been suggested that the isotropic chemical shielding at the phosphorus nucleus is directly related to the C−P−C bond angle in alkyldiphosphine disulfides.[15] With the characterization of the phosphorus chemical shift tensor in TMPS, this correlation can be examined more rigorously. Table 7 lists the phosphorus chemical shift data and the C−P−C bond angle for $[R_2P(S)]_2$ where R = methyl (this work), ethyl,[6] *n*-propyl,[44] or *n*-butyl.[17] It is difficult to draw any definite conclusion based on the first three compounds in the series, partly due to the experimental uncertainty in the C−P−C bond angle; however, it appears that the isotropic shielding trend does not follow the bond angle, i.e., increasing bond angle does not correlate directly with an increase in the isotropic chemical shift. Attempts have also been made to explain the difference between the phosphorus chemical shift for R = *n*-propyl and R = *n*-butyl by an effect similar to the γ-effect in ^{13}C NMR.[14b] We maintain that trends in the principal components of the phosphorus shift tensors must be considered, as has been done, for example, in the case of the dithiaphosphetanes, $[RSP(S)S]_2$ (R = alkyl or aryl).[18] For the alkyldiphosphine disulfides, the limited data available on the phosphorus chemical shift tensors (Table 7) indicate that the intermediate component, δ_{22}, changes the most (by about 23 ppm) upon going from R = methyl to R = ethyl. The least shielded component changes by about 17 ppm and the most shielded component by about 7 ppm. By contrast, all the principal components are similar for R = ethyl compared to R = *n*-butyl. Unfortunately, no data on the phosphorus chemical shift tensor are available for R = *n*-propyl.

Conclusions

The characterization of the phosphorus chemical shift and spin−spin coupling tensors for TMPS presented in this paper serves as a benchmark study for the evaluation of experimental NMR powder methods as well as the reliability of ab initio methods. The excellent agreement between the calculated and experimental phosphorus chemical shift tensor orientations is particularly encouraging. In TMPS, as in tetraethyldiphosphine disulfide,[6] the anisotropy in the *J*-coupling tensor is probably small. For TMPS, the upper limit in ΔJ is about 450 Hz. A number of alkyldiphosphine disulfides have been characterized by NMR, and attempts have been made to account for trends in the isotropic phosphorus chemical shifts; however, it is clear that the entire phosphorus chemical shift tensor must be considered. In addition, the structural data available in the literature for alkyldiphosphine disulfides are limited, and hence correlations between a particular structural feature in this class of compounds and the phosphorus chemical shifts are tenuous at best.

Acknowledgment. We are grateful to the solid-state NMR group at Dalhousie University for many helpful comments and suggestions, in particular Mike Lumsden for help with the analysis of the single-crystal NMR data. We also thank Brian Millier for his help with the maintenance of our spectrometers. R.E.W. thanks the Natural Sciences and Engineering Research Council (NSERC) of Canada for operating and equipment grants and the Canada Council for a Killam Research Fellowship. M.G. acknowledges NSERC, the Izaak Walton Killam Trust, and the Walter C. Sumner Foundation for postgraduate scholarships. All NMR spectra were acquired at the Atlantic Region Magnetic Resonance Centre (ARMRC), which is also supported by NSERC.

References and Notes

(1) (a) Eichele, K.; Wasylishen, R. E.; Nelson, J. H. *J. Phys. Chem. A* **1997**, *101*, 5463. (b) Vosegaard, T.; Skibsted, J.; Jakobsen, H. J. *J. Phys. Chem. A* **1999**, *103*, 9144.

(2) Jameson, C. J. *Annu. Rev. Phys. Chem.* **1996**, *47*, 135.

(3) Dixon, K. R. In *Multinuclear NMR*; Mason, J., Ed.; Plenum Press: New York, 1987; p 369.

(4) (a) VanderHart, D. L.; Gutowsky, H. S. *J. Chem. Phys*. **1968**, *49*, 261. (b) Zilm, K. W.; Grant, D. M. *J. Am. Chem. Soc*. **1981**, *103*, 2913. (c) Wasylishen, R. E.; Curtis, R. D.; Eichele, K.; Lumsden, M. D.; Penner, G. H.; Power, W. P.; Wu, G. In *Nuclear Magnetic Shieldings and Molecular Structure*; Tossell, J. A. Ed.; Kluwer Academic Publishers: Dordrecht, The Netherlands, 1993; p 297. (d) Wu, G.; Wasylishen, R. E. *Solid State Nucl. Magn. Reson.* **1995**, *4*, 47.

(5) (a) Eichele, K.; Ossenkamp, G. C.; Wasylishen, R. E.; Cameron, T. S. *Inorg. Chem*. **1999**, *38*, 639. (b) Bernard, G. M.; Wu, G.; Lumsden, M. D.; Wasylishen, R. E.; Maigrot, N.; Charrier, C.; Mathey, F. *J. Phys. Chem. A* **1999**, *103*, 1029. (c) Bernard, G. M.; Wu, G.; Wasylishen, R. E. *J. Phys. Chem. A* **1998**, *102*, 3184.

(6) Eichele, K.; Wu, G.; Wasylishen, R. E.; Britten, J. F. *J. Phys. Chem.* **1995**, *99*, 1030.

(7) Eichele, K.; Wasylishen, R. E. *J. Magn. Reson. A* **1994**, *106*, 46.

(8) Zilm, K. W.; Webb, G. G.; Cowley, A. H.; Pakulski, M.; Orendt, A. *J. Am. Chem. Soc*. **1988**, *110*, 2032.

(9) (a) Nakai, T.; McDowell, C. A. *J. Am. Chem. Soc.* **1994**, *116*, 6373. (b) Nakai, T.; McDowell, C. A. *Solid State Nucl. Magn. Reson.* **1995**, *4*, 163.

(10) (a) Iuliucci, R. J.; Phung, C. G.; Facelli, J. C.; Grant, D. M. *J. Am. Chem. Soc*. **1996**, *118*, 4880. (b) Iuliucci, R. J.; Phung, C. G.; Facelli, J. C.; Grant, D. M. *J. Am. Chem. Soc*. **1998**, *120*, 9305. (c) Schurko, R. W.; Wasylishen, R. E.; Foerster, H. *J. Phys. Chem. A* **1998**, *102*, 9750. (d) Bryce, D. L.; Wasylishen, R. E. *J. Phys. Chem. A* **1999**, *103*, 7364.

(11) (a) Chesnut, D. B. *Annu. Rep. NMR Spectrosc.* **1994**, *29*, 71. (b) de Dios, A. C. *Prog. NMR Spectrosc.* **1996**, *29*, 229. (c) Fukui, H. *Prog. NMR Spectrosc.* **1997**, *31*, 317. (d) Schreckenbach, G.; Ziegler, T. *Theor. Chem. Acc.* **1998**, *99*, 71. (e) Jameson, C. J. In *Nuclear Magnetic Resonance−A Specialist Periodical Report*; Webb, G. A., Ed.; Royal Society of Chemistry: Cambridge, UK, 1999; Vol. 28, p 42. (f) Helgaker, T.; Jaszuński, M.; Ruud, K. *Chem. Rev.* **1999**, *99*, 293. (g) *Modeling NMR Chemical Shifts: Gaining Insights into Structure and Environment*; Facelli, J. C., de Dios, A. C., Eds.; ACS Symposium Series 732; American Chemical Society: Washington, DC, 1999.

(12) (a) Santos, R. A.; Harbison, G. S. *J. Am. Chem. Soc*. **1994**, *116*, 3075. (b) Lumsden, M. D.; Wasylishen, R. E.; Britten, J. F. *J. Phys. Chem.* **1995**, *99*, 16602.

(13) Vosegaard, T.; Hald, E.; Langer, V.; Skov, H. J.; Daugaard, P.; Bildsøe, H.; Jakobsen, H. J. *J. Magn. Reson.* **1998**, *135*, 126.

(14) (a) Aime, S.; Harris, R. K.; McVicker, E. M.; Fild, M. *J. Chem. Soc., Dalton Trans.* **1976**, 2144. (b) Sarikahya, F.; Sarikahya, Y.; Topaloğu, I.; Şentürk, O. *Chim. Acta Turcica* **1997**, *25*, 35.

(15) Harris, R. K.; Merwin, L. H.; Hägele, G. *J. Chem. Soc., Faraday Trans. 1* **1987**, *83*, 1055.

(16) Tutunjian, P. N.; Waugh, J. S. *J. Chem. Phys.* **1982**, *76*, 1223.

(17) Tutunjian, P. N.; Waugh, J. S. *J. Magn. Reson.* **1982**, *49*, 155.

(18) (a) Krüger, K.; Grossmann, G.; Fleischer, U.; Franke, R.; Kutzelnigg, W. *Magn. Reson. Chem.* **1994**, *32*, 596. (b) Ohms, G.; Fleischer, U.; Kaiser, V. *J. Chem. Soc., Dalton Trans.* **1995**, 1297.

(19) Grimmer, A.-R.; Peter, R.; Fechner, E. *Z. Chem.* **1977**, *18*, 109.

(20) (a) SADABS, Sheldrick, G. M.; Bruker AXS, Inc., Madison, Wisconsin, 53719 USA. (b) Blessing, R. *Acta Crystallogr.* **1995**, *A51*, 33.

(21) Dutta, S. N.; Woolfson, M. M. *Acta Crystallogr.* **1961**, *14*, 178.

(22) SHELXTL (5.10) program library; Sheldrick, G., Siemens XRD, Madison WI.

(23) Rollett, J. S. *Computational Methods in Crystallography*; Pergamon Press: New York, 1975.

(24) Prince, E. *Mathematical Techniques in Crystallography and Materials Science*; Springer-Verlag: Berlin, 1994.

(25) (a) Kennedy, M. A.; Ellis, P. D. *Concepts Magn. Reson.* **1989**, *1*, 35. (b) Kennedy, M. A.; Ellis, P. D. *Concepts Magn. Reson.* **1989**, *1*, 109. (c) Eichele, K.; Chan, J. C. C.; Wasylishen, R. E.; Britten, J. F. *J. Phys. Chem. A* **1997**, *101*, 5423.

(26) Alderman, D. W.; Solum, M. S.; Grant, D. M. *J. Chem. Phys.* **1986**, *84*, 3717.

(27) Sun, B.; Griffin, R. G., unpublished results.

(28) Rance, M.; Byrd, R. A. *J. Magn. Reson.* **1983**, *52*, 221.

(29) *Gaussian 98*, Revision A.4; Frisch, M. J.; Trucks, G. W.; Schlegel, H. B.; Scuseria, G. E.; Robb, M. A.; Cheeseman, J. R.; Zakrzewski, V. G.; Montgomery, J. A., Jr.; Stratmann, R. E.; Burant, J. C.; Dapprich, S.; Millam, J. M.; Daniels, A. D.; Kudin, K. N.; Strain, M. C.; Farkas, O.; Tomasi, J.; Barone, V.; Cossi, M.; Cammi, R.; Mennucci, B.; Pomelli, C.; Adamo, C.; Clifford, S.; Ochterski, J.; Petersson, G. A.; Ayala, P. Y.; Cui, Q.; Morokuma, K.; Malick, D. K.; Rabuck, A. D.; Raghavachari, K.; Foresman, J. B.; Cioslowski, J.; Ortiz, J. V.; Stefanov, B. B.; Liu, G.; Liashenko, A.; Piskorz, P.; Komaromi, I.; Gomperts, R.; Martin, R. L.; Fox, D. J.; Keith, T.; Al-Laham, M. A.; Peng, C. Y.; Nanayakkara, A.; Gonzalez, C.; Challacombe, M.; Gill, P. M. W.; Johnson, B.; Chen, W.; Wong, M. W.; Andres, J. L.; Gonzalez, C.; Head-Gordon, M.; Replogle, E. S.; Pople, J. A. Gaussian, Inc.: Pittsburgh, PA, 1998.

(30) (a) Ditchfield, R. *Mol. Phys.* **1974**, *27*, 789. (b) Wolinski, K.; Hinton, J. F.; Pulay, P. *J. Am. Chem. Soc*. **1990**, *112*, 8251. (c) Rauhut, G.; Puyear, S.; Wolinski, K.; Pulay, P. *J. Phys. Chem.* **1996**, *100*, 6310.

(31) Jameson, C. J.; de Dios, A. C.; Jameson, A. K. *Chem. Phys. Lett.* **1990**, *167*, 575.

(32) Haeberlen, U. In *Advances in Magnetic Resonance*; Waugh, J. S., Ed.; Academic Press: New York, 1976; Supplement 1.

(33) Wasylishen, R. E. In *The Encyclopedia of NMR*; Grant, D. M., Harris, R. K., Eds.; John Wiley and Sons: New York, 1996; p 1685.

(34) (a) van Willigen, H.; Griffin, R. G.; Haberkorn, R. A. *J. Chem. Phys.* **1977**, *67*, 5855. (b) Power, W. P.; Wasylishen, R. E. *Annu. Rep. NMR Spectrosc.* **1991**, *23*, 1. (c) Curtis, R. D.; Hilborn, J. W.; Wu, G.; Lumsden, M. D.; Wasylishen, R. E.; Pincock, J. A. *J. Phys. Chem.* **1993**, *97*, 1856. (d) Lumsden, M. D.; Wu, G.; Wasylishen, R. E.; Curtis, R. D. *J. Am. Chem. Soc.* **1993**, *115*, 2825.

(35) Mason, J. *Solid State Nucl. Magn. Reson.* **1993**, *2*, 285.

(36) (a) Millar, J. M.; Thayer, A. M.; Zax, D. B.; Pines, A. *J. Am. Chem. Soc.* **1986**, *108*, 5113. (b) Nakai, T.; Ashida, J.; Terao, T. *Mol. Phys.* **1989**, *67*, 839.

(37) Lee, J. D.; Goodacre, G. W. *Acta Crystallogr.* **1971**, *B27*, 302.

(38) Ishii, Y.; Terao, T.; Hayashi, S. *J. Chem. Phys.* **1997**, *107*, 2760.

(39) Herzfeld, J.; Berger, A. E. *J. Chem. Phys.* **1980**, *73*, 6021.

(40) Wasylishen, R. E.; Power, W. P.; Penner, G. H.; Curtis, R. D. *Can. J. Chem.* **1989**, *67*, 1219.

(41) Schmidt-Rohr, K.; Spiess, H. W. *Multidimensional Solid-State NMR and Polymers*; Academic Press: London, 1994; p 444.

(42) Jameson, C. J. *Bull. Magn. Reson.* **1980**, *3*, 3.

(43) Bernard, G. M.; Wasylishen, R. E., unpublished results.

(44) Sillanpää, R.; Ergin, Ö.; Çelebi, S. *Acta Crystallogr.* **1993**, *C49*, 767.